Multiparametric Radiomics-Informed Transformer Framework for Autism Spectrum Disorder Diagnosis

No Author Given

No Institute Given

Abstract. Autism Spectrum Disorder (ASD) is one of the leading neurodevelopmental disorders in the world and rapidly increasing in prevalence. Existing automated ASD prediction systems have two critical drawbacks. The first one involves making the prediction using only Corpus Callosum (CC) segmentation data, whereas since similar changes are seen in other mental illnesses like schizophrenia and bipolar disorder, the CC segmentation is not enough to predict ASD. The second issue is that single parameteric from neuroimaging data; such as volume, area, or fiber integrity; cannot fully capture the intricate neuropathological changes in the CC associated with ASD development. There is no multiparametric-based radiomics learning model that is based solely on a single ROI. To address these limitations, we propose a radiomics-informed transformer framework for detecting ASD from a single ROI-based radiomics extracted features. The proposed framework operates through two key mechanisms. First, we have developed an optimized hidden Markov random field algorithm for CC segmentation that addresses resource constraints by focusing exclusively on the localized region of the CC. Second, we leverage BERT to distinguish radiomic features of healthy and ASD subjects. Furthermore, we ensure complementary information is learned by tokenized radiomics and radiomic features by designing an effective feature de-correlation loss. Combined, our method addresses the limitations of ASD diagnosis, achieving 98.2% DSC for CC segmentation and 96.8% for the ASD classification task.

Keywords: Corpus Callosum · Autism Spectrum Disorder · Radiomics.

1 Introduction

Autism Spectrum Disorder (ASD) is a neurodevelopmental condition affecting communication, social interaction, and behavior [1]. Diagnosing ASD is challenging due to the lack of definitive medical tests, relying instead on behavioral and developmental assessments [2]. Structural and functional abnormalities in the Corpus Callosum (CC), which facilitates interhemispheric communication, are linked to ASD symptoms [3], [4], [5], [6]. Notably, a decreased size of the CC is consistently observed in individuals with ASD [3]. Identifying structural biomarkers for ASD is clinically important, and this paper aims to propose and

validate an automated approach using Radiomics-Informed Transformers (RIT), is illustrated in Fig. 1 to detect CC abnormalities, potentially enhancing early diagnosis and intervention strategies.

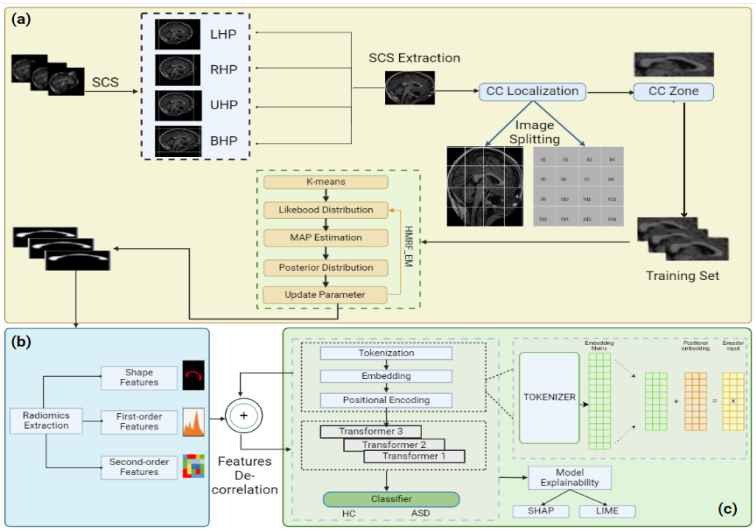

Fig. 1: Overview of our method.(a) CC Localization and segmentation. (b) Radiomics feature extraction. (c) Encouraging complementary radiomic features through Feature de-correlation in RIT.

In the literature, studies typically either focus only on segmenting the CC or on the global detection of ASD from MRI (fMRI) scans. For instance, the UNet model has been adopted for the CC segmentation [7], while employing different data augmentation techniques. Furthermore, a comparative study implemented and evaluated three different DL models: CENet, UNet++, and MultiResUNet [8]. Recently, Chandra et al. proposed a U-Net-based Fully Convolutional Network for automatic CC segmentation (CCsNeT) in brain MRI images [9]. A recent study employed a dual deep-learning classifiers approach for CC segmentation, using bidirectional LSTM with CBAM and a Modified Convolutional Neural Network (M-CNN) to enhance accuracy [10]. However, these methods are limited to segmentation tasks without offering diagnostic capabilities. Additionally, the effectiveness of these deep learning models is often hindered by the lack of available data, which restricts their accuracy and generalizability. On the other hand, the Federated Learning (FL) technique was uniquely applied for autism detection by locally training two different machine learning classifiers, logistic regression and support vector machine [11]. These classifiers were used to classify ASD factors and detect ASD in both children and adults. Perochon et al. proposed an application that displayed stimuli designed to elicit behavioral

signs of autism, which were quantified using computer vision and machine learning techniques [12]. These behavioral signs were analyzed to train the XGBoost model which aimed at distinguishing between diagnostic groups. Furthermore, a novel method called Com-BrainTF introduced a hierarchical local-global transformer architecture to learn intra- and inter-community aware node embeddings for the ASD prediction task [13]. Although these methods propose different ways of using both approaches, *they do not address the limitations of either focusing solely on CC segmentation or on global ASD detection nor do they explore ways to combine their complementary advantages.*

However, neuroimaging measures of the CC are not diagnostic of autism, as similar alterations are found in disorders like schizophrenia and bipolar disorder [14]. Single-value parameters from neuroimaging data do not capture the complex neuropathological changes in the CC associated with autism. Autism's pathogenesis involves microscopic alterations in brain tissue from various genetic, molecular, and cytoarchitectural factors. Therefore, an approach that quantifies the spatial distribution of microscopic tissue heterogeneity could improve autism diagnosis. Radiomics uncover meaningful information within radiological images, offering deeper insights into tissue characteristics beyond single-value approaches [15]. This technique, applied to segmented CC data, has the potential for enhancing ASD detection by extracting a comprehensive array of quantitative features, including texture, shape, intensity, and spatial relationships within tissues.

In this work, we propose an approach for detecting ASD by integrating radiomic and transformer-based deep learning methods from segmented CC scans. Radiomic features are calculated locally around each voxel. Traditionally independent, these features show interdependencies reflecting biological processes and spatial relationships within tissues. Thus, our key contributions are:

- We localize and extract the CC from brain MRIs by defining a square around the skull, and isolating the CC-containing region. To address resource constraints in low-income settings, we use an optimized Hidden Markov Random Field (HMRF) algorithm for computationally efficient CC segmentation.
- We integrate radiomic features with a transformer-based deep learning model, tokenizing the features using BERT for nuanced representation.
- We enhance the segmentation process by integrating tokenized radiomic features and enforcing feature de-correlation, ensuring precise and complementary feature extraction. To our knowledge, no study has tested an ASD diagnostic model using radiomics focused on interhemispheric connectivity.

2 Methodology

In this study, ASD detection is structured as a multistage process focusing on single region analysis, specifically the CC, which exhibits significant importance for radiomics analysis. To optimize CC localization from brain MRIs, we have developed a method that includes sub-image division and an HMRF algorithm. This approach is specifically designed to accommodate resource-constrained settings.

2.1 CC Localization and Segmentation

The proposed approach consists of (a) identifying the square circumscribing skull and (b) dividing this square into 16 equal regions $(R_1, R_2, \ldots, R_{16})$, aiming to find the local minimum region that contains the CC.

Square Circumscribing Skull

In this study, we introduce a method for segmenting the CC while addressing the challenge of reducing the segmentation zone. The approach divides the Square Circumscribing Skull (SCS) into a grid of 4 rows and 4 columns to localize the skull within the original matrix M. After slicing, we obtain 16 sub-images. Evaluation with 1000 MRIs showed that 90% of the CC overlaps with the union of R_6 and R_7.

To localize the CC more precisely, we use $ccROI$ as the seed and expand it to $\widetilde{ccROI}_\epsilon$, defined as:

$$\widetilde{ccROI}_\epsilon = SCS\left[\frac{n_s}{4} - \epsilon : \frac{n_s}{2} + \epsilon, \frac{m_s}{4} - \epsilon : \frac{3}{4}m_s + \epsilon\right] \tag{1}$$

The expansion parameter ϵ is crucial but lacks a predefined statistical method. We employ an iterative approach to find the optimal ϵ, aiming to maximize the percentage p_ϵ of CC contained within $\widetilde{ccROI}_\epsilon$. The Elbow method helps determine ϵ by plotting p_ϵ against ϵ values and identifying the optimal point where further expansion does not significantly increase p_ϵ.

Algorithm Overview The optimized HMRF algorithm leverages the spatial dependencies and intensity characteristics within the SCS sub-images to refine the segmentation of the CC (**Algorithm 1**).

Algorithm 1 Optimized HMRF Algorithm

Require: SCS: Square Circumscribing Skull sub-image
Ensure: Segmented CC region CC_{seg}
Initialize HMRF parameters and pixel labels
repeat
  Update pixel labels using local neighborhood information:
  $L(i) \leftarrow \arg\max P(L(i) = l | x(i), \mathbf{W})$
  where $L(i)$ is the label of pixel i, $x(i)$ denotes the feature vector at pixel i, and $\mathbf{W}$ represents model parameters.
  Refine labels based on global image properties:
  $P(L(i) = l|\mathbf{W}) \propto \exp\left(\sum_{j\in\mathcal{N}(i)} \lambda_{ij}\delta(L(i), L(j)) + \gamma_i(l)\right)$
  where λ_{ij} captures pairwise interactions between neighboring pixels and γ_i encodes unary potentials.
until Convergence criteria are met
Extract CC_{seg} from the final pixel labels

2.2 Radiomics feature extraction

Radiomics is an analytical technique that allows for the computation of multiple descriptors of shape and texture [16]. The relevant information present in the image is extracted using three classes of features: (i) shape features, (ii) first-order features, and (iii) texture-based features. In fact, texture features are designed to capture local variations in the image, utilizing measures such as Gray-level Co-occurrence Matrices (GLCM) to represent second-order textural distributions. Conventional statistical metrics, including entropy and correlation, are commonly employed to summarize these textural measures [17]. Recently, brain radiomics features have been used to understand neurodegenerative conditions such as schizophrenia [18], revealing patterns invisible to the naked eye. However, there are no existing reports of clinical models based on CC radiomics features, likely due to the absence of appropriate datasets. Radiomic feature extraction from the segmented CC was performed using py-Radiomics (version 3.1.0; https://pyradiomics.readthedocs.io/en/latest/) [19], which conformed to the Image Biomarker Standardization Initiative [20].

2.3 Encouraging Complementary Radiomic Features through Feature De-correlation in RIT

Unlike existing classification approaches that rely on generic radiomic features or deep learning models, our method leverages the power of tokenization to enhance feature representation. Traditional methods often suffer from limitations such as naive feature concatenation, which fails to capture the complex interdependencies within the data. In contrast, our approach integrates tokenized radiomic features using BERT, producing token embeddings that are directly used in the classification task. To enforce learning of complementary features, we introduce a de-correlation loss between BERT token embeddings Z_i and original radiomic features R_i:

$$L_{\text{corr}} = \left\| \frac{\sum_{i=1}^{N_k} w^i Z_i^T R_i}{\sum_{i=1}^{N_k} w^i} \right\| \tag{2}$$

Where T_i represents the token embeddings from BERT R_i represents the radiomic features w^i is the exponential weighting parameter N_k is the number of features stored in the feature bank.

3 Experiments

3.1 Datasets

The experiment investigated two datasets: the Autism Brain Imaging Data Exchange (ABIDE) and a dataset collected from the Military Hospital of Tunis in Tunisia. We noticed a lack of publicly available GT for CC segmentation within

the widely used datasets. The ABIDE dataset includes two large-scale collections, ABIDE I and ABIDE II. ABIDE I contains 1112 scans, with 539 from individuals with ASD and 573 from HC. ABIDE II includes 1114 scans from 521 individuals with ASD and 593 HC. Additionally, we used a private dataset of 101 patients from the Military Hospital of Tunis, consisting of 74 ASD cases and 27 HC. A professional neurologist manually segmented the CC regions from the images, creating a valuable GT for CC segmentation.

3.2 Qualitative and Quantitative Results

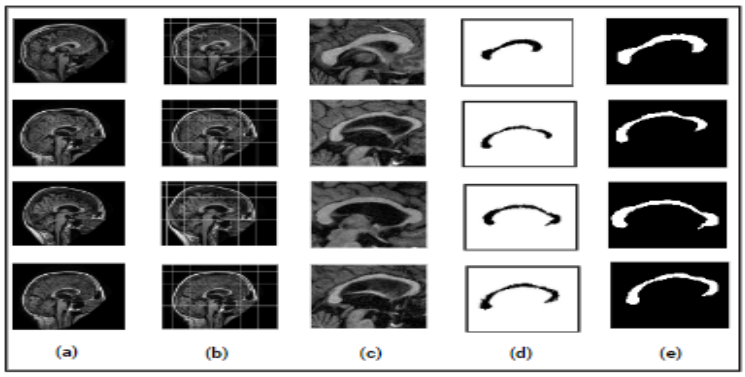

Fig. 2: Qualitative results.(a) Input MRI from ABIDE. (b) Mapped MRI. (c) Cropped MRI. (d) GT. (e) Optimized HMRF (Ours)

Fig. 2 demonstrates the visual evaluation of the results obtained from challenging brain MRI scans, confirming the accuracy of our proposed method for CC segmentation. Our collaborating clinician expert has verified that the CC shape and thickness are clearly defined, and the delineated CC area closely aligns with the four anatomical divisions of the CC, particularly delineating critical areas like the rostrum and splenium. Importantly, the fornix is accurately excluded from the CC area. The method successfully extracts the CC from both ASD (cases 1 and 3) and HC (cases 2 and 4) subjects. Specifically, the method effectively distinguishes CC from neighboring tissues of similar intensity, resolving this challenge within the MRI examples provided.

Proposed Method versus experts in a Turing-like test Radiologist and neurologist from the Military Hospital of Tunis independently assessed the quality of CC masks generated either by human experts or the optimized HMRF algorithm. Each expert evaluated 50 scans with annotated slices, which were randomized to ensure unbiased assessment. The clinicians were blinded to whether the CC masks were generated by humans or the algorithm, and they rated the completeness of the segmented CC and the correctness of its contours on a 1-6

scale. In over 30 images, experts consistently selected the GT as exhibiting the best delineation, while in 10 images, our method closely resembled the GT to such an extent that experts were unable to distinguish between them.

Quantitative Comparison with State-of-the-art for CC segmentation In Table 1 we compare our method against the relevant deep learning methods, as well as baseline [8], [9], [10]. According to the Dice Similarity Coefficients (DSC), we can see that we have reached our goal by making higher scores with 98.2% comparatively to relevant deep learning methods. Likewise, we have recorded high Accuracy scores (Acc) with 99.6%. On the other hand, for sensitivity metric, the proposed method reaches good score and still better than CCsNeT [9] and Optimized UNet [10] methods. The decline of the proposed method performance according to this metric can be explained by the cause of the GT which is manually drawing.

Table 1: Comparison with state-of-the-art methods for CC segmentation. Baseline†is a naïve CC segmentation implementation using basic HMRF.

Method	Model	DSC (%)	Acc (%)	Specificity (%)
Shrivastava et al.[8]	UNet++	71.68	99.36	99.44
Shrivastava et al.[8]	CE-Net	93.11	99.89	**99.94**
Shrivastava et al.[8]	MultiResUNet	80.2	79.71	79.55
Chandra et al. [9]	CCsNeT	96.74	-	-
Padmanabha Sarma and Saranya [10]	Optimized UNet	97.81	96.28	98.83
Baseline†	HMRF	86.3	91.3	93.47
Proposed Method	**Optimized HMRF**	**98.2**	**99.6**	94.9

Quantitative Comparison with State-of-the-art for ASD classification As seen in Table 2 , our proposed RIT model outperforms all other architectures. Notably, it achieves the highest accuracy at 96.8% and precision at 83.1 %. While Com-BrainTF demonstrates superior sensitivity (80.1 %).

Table 2: Comparison with state-of-the-art methods for ASD classification.

Method	Model	Acc (%)	Sensitivity (%)	Precision (%)
Farooq et al.[11]	SVM	81	✗	81
Farooq et al.[11]	LR	78	✗	73
Bannadabhavi et al.[13]	Com-BrainTF	72.5	**80.1**	✗
Proposed Method	**RIT**	**96.8**	72.3	**83.1**

3.3 Ablation Study

Effect of Square Circumscribing Skull and Localization In Table 3, we present an ablation study to evaluate the impact of using the SCS and local-

ization on the performance of our proposed method. The first baseline model, which does not use SCS or localization, achieves a Dice DSC of 79.2%. Incorporating localization but not SCS in the second baseline model improves the DSC to 82.11%. The third baseline model, which employs both SCS and localization, shows a significant improvement with a DSC of 95.6%.

Table 3: Ablation study for proposed method of CC segmentation.

Model	SCS	Localization	Nb_Class	DSC (%)	Acc (%)
Baseline†	✗	✗	Manually	79.2	65.3
Baseline †	✓	✗	Manually	82.11	80.52
Baseline†	✓	✓	Manually	95.6	98.1
Optimized HMRF	✓	✓	Automatic	99.2	99.6

Effectiveness of tokenized radiomic feature and de-correlation We perform ablation experiments to demonstrate improvements from using radiomic features, tokenized radiomic features, and feature de-correlation loss. Results are shown in Table 4. We can see that including feature de-correlation further boosts performance and leads to the best overall results.

Table 4: Ablation study for proposed method of ASD classification.

Model	R_i	T_i	L_{corr}	Acc (%)
Baseline†	✓	✗	✗	75.9
Baseline †	✗	✓	✗	81.26
RIT	✓	✓	✓	96.8

4 Conclusion

In this work, we propose a new approach for CC segmentation from brain MRIs based on radiomic and deep learning techniques. Our method is based on two key ideas: precise localization of the CC by defining a square around the skull and isolating the CC-containing region, and enhancing feature representation through tokenization and feature de-correlation. Unlike existing approaches, our method specifically addresses the computational constraints in low-resource settings and improves feature extraction. We achieve state-of-the-art results in both CC segmentation and ASD classification, outperforming existing methods. Additionally, we have explored the diagnostic potential of our approach for ASD by investigating the interhemispheric connectivity captured in the CC. Our future work includes investigating more sophisticated radiomic feature and larger datasets.

References

1. Chien, Y. L., Wu, C. S., and Tsai, H. J. (2021). The comorbidity of schizophrenia spectrum and mood disorders in autism spectrum disorder. Autism Research, 14(3), 571-581.
2. McCarty, P., and Frye, R. E. (2020, October). Early detection and diagnosis of autism spectrum disorder: Why is it so difficult?. In Seminars in Pediatric Neurology (Vol. 35, p. 100831). WB Saunders.
3. Valenti, M., Pino, M. C., Mazza, M., Panzarino, G., Di Paolantonio, C., Verrotti, A. (2020). Abnormal structural and functional connectivity of the corpus callosum in autism spectrum disorders: A review. Review Journal of Autism and Developmental Disorders, 7, 46-62.
4. Loomba, N., Beckerson, M. E., Ammons, C. J., Maximo, J. O., Kana, R. K. (2021). Corpus callosum size and homotopic connectivity in autism spectrum disorder. Psychiatry Research: Neuroimaging, 313, 111301.
5. Paul, L. K., Corsello, C., Kennedy, D. P., Adolphs, R. (2014). Agenesis of the corpus callosum and autism: a comprehensive comparison. Brain, 137(6), 1813-1829.
6. Kennedy, D. P., Paul, L. K., Adolphs, R. (2015). Brain connectivity in autism: the significance of null findings. Biological Psychiatry, 78(2), 81-82.
7. Chandra, A., Verma, S., Raghuvanshi, A. S., Londhe, N. D., Bodhey, N. K., Subham, K. (2019, February). Corpus callosum segmentation from brain mri and its possible application in detection of diseases. In 2019 IEEE International Conference on Electrical, Computer and Communication Technologies (ICECCT) (pp. 1-4). IEEE.
8. Shrivastava, S., Singh, N., Mishra, U., Chandra, A., Verma, S. (2020, March). Comparative study of deep learning models for segmentation of corpus callosum. In 2020 Fourth International Conference on Computing Methodologies and Communication (ICCMC) (pp. 418-423). IEEE.
9. Chandra, A., Verma, S., Raghuvanshi, A. S., Bodhey, N. K. (2022). CCsNeT: Automated Corpus Callosum segmentation using fully convolutional network based on U-Net. Biocybernetics and Biomedical Engineering, 42(1), 187-203.
10. Padmanabha Sarma, A., Saranya, G. (2023). Segmentation of the Corpus Callosum from Brain Magnetic Resonance Images Using Dual Deep Learning Classifiers and Optimized U-Shaped Neural Networks. SN Computer Science, 5(1), 1.
11. Farooq, M. S., Tehseen, R., Sabir, M., Atal, Z. (2023). Detection of autism spectrum disorder (ASD) in children and adults using machine learning. Scientific Reports, 13(1), 9605.
12. Perochon, S., Di Martino, J. M., Carpenter, K. L., Compton, S., Davis, N., Eichner, B., ... Dawson, G. (2023). Early detection of autism using digital behavioral phenotyping. Nature Medicine, 29(10), 2489-2497.
13. Bannadabhavi, A., Lee, S., Deng, W., Ying, R., Li, X. (2023, October). Community-Aware Transformer for Autism Prediction in fMRI Connectome. In International Conference on Medical Image Computing and Computer-Assisted Intervention (pp. 287-297). Cham: Springer Nature Switzerland.
14. Bang, M., Eom, J., An, C., Kim, S., Park, Y. W., Ahn, S. S., ... Lee, S. H. (2021). An interpretable multiparametric radiomics model for the diagnosis of schizophrenia using magnetic resonance imaging of the corpus callosum. Translational psychiatry, 11(1), 462.
15. Scapicchio, C., Gabelloni, M., Barucci, A., Cioni, D., Saba, L., Neri, E. (2021). A deep look into radiomics. La radiologia medica, 126(10), 1296-1311.

16. Lambin, P., Leijenaar, R. T., Deist, T. M., Peerlings, J., De Jong, E. E., Van Timmeren, J., ... Walsh, S. (2017). Radiomics: the bridge between medical imaging and personalized medicine. Nature reviews Clinical oncology, 14(12), 749-762.
17. Zwanenburg, A., Vallières, M., Abdalah, M. A., Aerts, H. J., Andrearczyk, V., Apte, A., ... Löck, S. (2020). The image biomarker standardization initiative: standardized quantitative radiomics for high-throughput image-based phenotyping. Radiology, 295(2), 328-338.
18. Bang, M., Eom, J., An, C., Kim, S., Park, Y. W., Ahn, S. S., ... Lee, S. H. (2021). An interpretable multiparametric radiomics model for the diagnosis of schizophrenia using magnetic resonance imaging of the corpus callosum. Translational psychiatry, 11(1), 462.
19. Van Griethuysen, J. J., Fedorov, A., Parmar, C., Hosny, A., Aucoin, N., Narayan, V., ... Aerts, H. J. (2017). Computational radiomics system to decode the radiographic phenotype. Cancer research, 77(21), e104-e107.
20. Zwanenburg, A., Vallières, M., Abdalah, M. A., Aerts, H. J., Andrearczyk, V., Apte, A., ... Löck, S. (2020). The image biomarker standardization initiative: standardized quantitative radiomics for high-throughput image-based phenotyping. Radiology, 295(2), 328-338.